A distributionally robust approach for mixed aleatory and epistemic uncertainties propagation

Masaru Kitahara [a, *], Jingwen Song [b], Pengfei Wei [c], Matteo Broggi [a], Michael Beer [a, d, e]

[a] *Leibniz Universität Hannover, Institute for Risk and Reliability, Callinstrasse 34, Hannover, Germany*

[b] *Northwestern Polytechnical University, State IJR center of Aerospace Design and Additive Manufacturing, Xi'an 710072, China*

[c] *Northwestern Polytechnical University, School of Mechanics, Civil Engineering and Architecture, Xi'an 710072, China*

[d] *University of Liverpool, Institute for Risk and Uncertainty, Peach Street L69 7ZF Liverpool, United Kingdom*

[e] *Tongji University, International Joint Research Center for Engineering Reliability and Stochastic Mechanics, Shanghai 200092, China*

* Correspondence author. E-mail address: masaru.kitahara@irz.uni-hannover.de (M. Kitahara).

Keywords:

Uncertainty quantification; Imprecise probabilities; Failure probability bounds; Sensitivity analysis; Staircase distributions

1. Introduction

Uncertainties are typically classified into aleatory and epistemic uncertainty [1], and uncertainty characterization models can be then categorized into the following three groups:

- Probability model is the most classical one, and is usually used to represent aleatory uncertainty;
- Non-probabilistic models [2] are set-theoretical models, and are especially suitable to characterize epistemic uncertainty;
- Imprecise probability models [3] are considered as a combination of the former two models, and can separately characterize aleatory and epistemic uncertainties.

Among the aforementioned models, effective propagation of the imprecise probability models has been intensively investigated in the past decades. The extended Monte Carlo simulation (EMCS) [4] is an importance sampling-based method relying on a single stochastic simulation. Therefore, its computational cost is the same as that for the conventional reliability analysis. Moreover, the method has been integrated with the high-dimensional model representation (HDMR) decomposition as the metamodel strategy and sensitivity analysis to measure the importance of the epistemic parameters, to establish a general methodology framework, called non-intrusive imprecise stochastic simulation (NISS) [5,6], and it has been also generalized to propagate the imprecise probability models and non-probabilistic models simultaneously [7].

However, the main drawback of the NISS framework is that it is restricted to the parameterized imprecise probability models, e.g., distributional p-boxes [8], which impose constraints on admissible distribution functions by assuming a specific distribution family. Comparatively, if the distribution families of the aleatory parameters cannot be determined a priori, it becomes necessary to propagate all the possible distributions of arbitral distribution families enclosed within a concerned p-box, so as to accurately estimate the failure probability bounds. Crespo et al. [9] has recently developed a novel distribution family, called staircase distribution, that can approximate a broad range of distributions arbitrary close. Whereas its applications in imprecise stochastic simulation are quite limited in current literatures, it has a potential to define a parametric p-box approximately containing any distributions within its bounds. The aim of this work is consequently to generalize the staircase distribution-based p-boxes and integrate them with the NISS method to develop a novel framework for propagating the imprecise probability models without limiting hypotheses on the distribution family.

The present work particularly focuses on the generalized global NISS method [7], because it can propagate both the imprecise probability models and non-probabilistic models at the same time. The staircase distributions are theoretically ready to be utilized in this method by constructing parametric p-boxes defining their hyper-parameters as interval values. However, it requires to parameterize the distribution function for a significant number of the hyper-parameters sets to derive NISS estimators. This can be computationally prohibitive for the staircase distributions whose density functions are parameterized by solving optimization problems. To address this issue, a novel hybrid NISS method is proposed, where the staircase distribution-based p-boxes are propagated by the local NISS method [5] whereas the non-probabilistic models, i.e., interval models, are propagated using the global NISS method [6]. The feasibility of the proposed method is demonstrated by solving the reliability analysis subproblem of the NASA UQ challenge problem 2019 [10].

2. Parametric p-boxes bases on staircase distributions

Staircase distributions [9] are functions of their hyper-parameters $\boldsymbol{\theta} = [\mu, m_2, \tilde{m}_3, \tilde{m}_4]$ consisting of the mean μ, variance m_2, skewness $\tilde{m}_3$, and kurtosis $\tilde{m}_4$. The PDF of a staircase random variable x on its support domain $[\underline{x}, \overline{x}]$ can be expressed as:

$$f_{\mathrm{x}}(x) = \begin{cases} l_i & \forall x \in (x^i, x^{i+1}], \text{for } 1 \le i \le n_b \\ 0 & \text{otherwise} \end{cases} \tag{1}$$

where $l_i (\ge 0)$ means the PDF value of the ith bin; $x^i = \underline{x} + (i-1)\kappa$, with the length $\kappa = (\overline{x} - \underline{x})/n_b$, denotes the ith left partitioning point; n_b is the number of bins. The PDF values l_i, for $1 \le i \le n_b$, can be obtained by solving an optimization problem based on the moment matching constraints, and one can refer to Ref. [9] for their detailed derivation. The staircase distribution can define a parametric p-box by CDF families the hyper-parameters of which are known in intervals:

$$F_{\mathrm{x}}(x) = F_{\mathrm{x}}(x|\boldsymbol{\theta}), \text{for } \boldsymbol{\theta} \in \{D_{\boldsymbol{\theta}} \cap \Theta\} \tag{2}$$

where $D_{\boldsymbol{\theta}}$ is the interval domain of $\boldsymbol{\theta}$; Θ means the feasible domain of $\boldsymbol{\theta}$ as moment constraints for the existence of x [9]. Without loss of generality, we assume the intervals are independent with each other and $D_{\boldsymbol{\theta}} = [\underline{\mu}, \overline{\mu}] \times [\underline{m}_2, \overline{m}_2] \times [\underline{\tilde{m}}_3, \overline{\tilde{m}}_3] \times [\underline{\tilde{m}}_4, \overline{\tilde{m}}_4]$ denotes a hyper-rectangular domain.

Fig.1 depicts an example of a parametric p-box consisting of a staircase distribution family with a support set $x \in [-5, 5]$, mean $\mu \in [-1, 1]$, variance $m_2 \in [0.8, 1.2]$, skewness $\tilde{m}_3 \in [-0.75, 0.75]$, and kurtosis $\tilde{m}_4 \in [2, 4]$, as well as a parametric p-box that consists of a Gaussian distribution family with the same intervals for the mean and variance as above. Moreover, four possible CDF realizations for each type of the p-box are shown in the figure. The Gaussian distribution-based p-box naturally only contains Gaussian distributions, while the staircase distribution-based p-box contains a broad range of distributions, including skewed and bi-modal distributions.

The staircase distribution-based p-box is capable of realizing arbitral distribution functions the hyper-parameters of which are in $\{D_{\boldsymbol{\theta}} \cap \Theta\}$, while it allows a clear separation of aleatory uncertainty, represented by distribution families, and epistemic uncertainty, represented by given intervals of the hyper-parameters. These properties fulfill the expectation as a parameterized imprecise probability model with no limiting hypothesis on the distribution family.

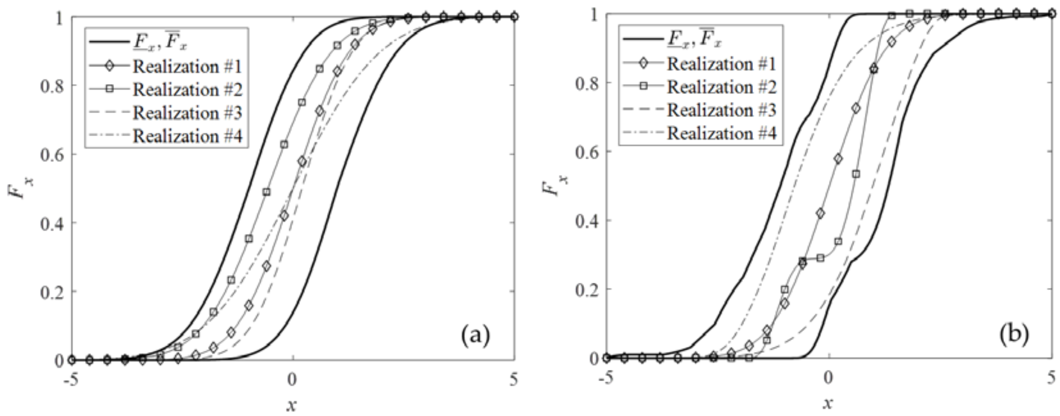

Fig. 1. Illustration of Gaussian distribution-based and staircase distribution-based p-boxes.

3. Hybrid NISS method

Suppose $g(\boldsymbol{x}, \boldsymbol{y})$ be the limit state function, where $\boldsymbol{x} = (x_1, x_2, \cdots, x_n)^T$ denotes the n-dimensional staircase random variables and $\boldsymbol{y} = (y_1, y_2, \cdots, y_m)^T \in D_{\boldsymbol{y}}$ is the m-dimensional independent interval parameters with the hyper-rectangular domain $D_{\boldsymbol{y}}$. Without loss of generality, we assume that $\boldsymbol{x}$ are independent to each other, so that the joint PDF is expressed as $f_{\mathbf{x}}(\boldsymbol{x}) = \prod_{i=1}^{n} f_{\mathrm{x}_i}(x_i|\mu_i, m_{2i}, \widetilde{m}_{3i}, \widetilde{m}_{4i})$, for $\boldsymbol{\mu} \in D_{\boldsymbol{\mu}}$, $\boldsymbol{m}_2 \in D_{\boldsymbol{m}_2}$, $\widetilde{\boldsymbol{m}}_3 \in D_{\widetilde{\boldsymbol{m}}_3}$, and $\widetilde{\boldsymbol{m}}_4 \in D_{\widetilde{\boldsymbol{m}}_4}$, where $\boldsymbol{\mu}$, $\boldsymbol{m}_2$, $\widetilde{\boldsymbol{m}}_3$ and $\widetilde{\boldsymbol{m}}_4$ are columns of the means, variances, skewnesses and kurtoses, respectively; $D_{\boldsymbol{\mu}}$, $D_{\boldsymbol{m}_2}$, $D_{\widetilde{\boldsymbol{m}}_3}$ and $D_{\widetilde{\boldsymbol{m}}_4}$ mean the hyper-rectangular domains of $\boldsymbol{\mu}$, $\boldsymbol{m}_2$, $\widetilde{\boldsymbol{m}}_3$ and $\widetilde{\boldsymbol{m}}_4$. Noted that, the independence assumption on $\boldsymbol{x}$ is not crucial for the proposed method. In fact, the dependence structure among the staircase random variables enables to be uniquely defined by a copula function [11], thus the following steps to derive the NISS estimators do almost not affected by the presence of dependent inputs. The above definition further brings $4n$-dimensional epistemic parameters $\boldsymbol{\vartheta} = (\mu_1, \cdots, \mu_n, m_{21}, \cdots, m_{2n}, \widetilde{m}_{31}, \cdots, \widetilde{m}_{3n}, \ \widetilde{m}_{41}, \cdots, \widetilde{m}_{4n})^T$, and their support set is the hyper-rectangular $D_{\boldsymbol{\vartheta}} = D_{\boldsymbol{\mu}} \times D_{\boldsymbol{m}_2} \times D_{\widetilde{\boldsymbol{m}}_3} \times D_{\widetilde{\boldsymbol{m}}_4}$. For convenience in notation, let $\boldsymbol{\vartheta} = (\vartheta_1, \ \cdots, \vartheta_{4n})^T$, where $\vartheta_i = \mu_i$, $\vartheta_{2i} = m_{2i}$, $\vartheta_{3i} = \widetilde{m}_{3i}$, and , $\vartheta_{4i} = \widetilde{m}_{4i}$, for $i = 1, \cdots, n$.

We assume that the failure happens when $g(\boldsymbol{x}, \boldsymbol{y}) < 0$ and the failure domain can be represented as $F = \{\boldsymbol{x}, \boldsymbol{y}\colon g(\boldsymbol{x}, \boldsymbol{y}) < 0\}$. The indicator function of F is then formulated by $I_F(\boldsymbol{x}, \boldsymbol{y}) = 1$ if $\{\boldsymbol{x}, \boldsymbol{y}\} \in F$, and else $I_F(\boldsymbol{x}, \boldsymbol{y}) = 0$. The failure probability function can be then expressed as:

$$P_f(\boldsymbol{\vartheta}, \boldsymbol{y}) = \int_{\mathbb{R}^n} I_F(\boldsymbol{x}, \boldsymbol{y}) f_{\mathbf{x}}(\boldsymbol{x}|\boldsymbol{\vartheta}) d\boldsymbol{x} \tag{3}$$

The HDMR decomposition of the failure probability function expresses $P_f(\boldsymbol{\vartheta}, \boldsymbol{y})$ as the sum of a series of component functions:

$$\begin{aligned} P_f(\boldsymbol{\vartheta}, \boldsymbol{y}) \approx P_{f0} &+ \sum_{i=1}^{4n} P_{f\vartheta_i}(\vartheta_i) + \sum_{i=1}^{m} P_{fy_i}(y_i) + \sum_{i=1}^{4n-1} \sum_{j=i+1}^{4n} P_{f\boldsymbol{\vartheta}_{ij}}(\boldsymbol{\vartheta}_{ij}) + \sum_{i=1}^{m-1} \sum_{j=i+1}^{m} P_{f\boldsymbol{y}_{ij}}(\boldsymbol{y}_{ij}) \\ &+ \sum_{i=1}^{4n} \sum_{j=1}^{m} P_{f\vartheta_i y_j}(\vartheta_i, y_j) + \cdots + P_{f\boldsymbol{\vartheta}\boldsymbol{y}}(\boldsymbol{\vartheta}, \boldsymbol{y}) \end{aligned} \tag{4}$$

where P_{f0} denotes the constant component; $P_{f\vartheta_i}$ and P_{fy_i} refer to the first-order component functions; $P_{f\boldsymbol{\vartheta}_{ij}}$, $P_{f\boldsymbol{y}_{ij}}$, and $P_{f\vartheta_i y_j}$ mean the second-order component functions; $\boldsymbol{\vartheta}_{ij}$ is the two-dimensional vector consisting of ϑ_i and ϑ_j, and $\boldsymbol{y}_{ij}$ possesses a similar structure for $\boldsymbol{y}$. It has been demonstrated that the HDMR decomposition with second-order truncation commonly leads to a satisfactory approximation of the failure probability function [6,7]. Thus, we do not go for the higher-order component functions in the rest part of this paper.

A hybrid NISS method is herein developed, where the staircase distribution-based p-boxes are propagated by the local NISS method [6] to significantly suppress the computational cost to estimate the component functions over the hyper-parameters, by performing the parameterizations of the joint PDFs at a single well-chosen point of $\boldsymbol{\vartheta}$. On the other hand, the interval models are propagated using the global NISS method [7] for maintaining the global accuracy of the estimators of the corresponding component functions. In this context, the HDMR component functions can be defined as:

$$\begin{cases} P_{f0} = \int P_f(\boldsymbol{\vartheta}^*, \boldsymbol{y}) f_{\mathbf{y}}(\boldsymbol{y}) d\boldsymbol{y} \\ P_{f\vartheta_i}(\vartheta_i) = \int P_f(\vartheta_i, \boldsymbol{\vartheta}^*_{-i}, \boldsymbol{y}) f_{\mathbf{y}}(\boldsymbol{y}) d\boldsymbol{y} \ - P_{f0} \\ P_{fy_i}(y_i) = \int P_f(\boldsymbol{\vartheta}^*, \boldsymbol{y}) f_{\mathbf{y}_{-i}}(\boldsymbol{y}_{-i}) d\boldsymbol{y}_{-i} \ - P_{f0} \\ P_{f\boldsymbol{\vartheta}_{ij}}(\boldsymbol{\vartheta}_{ij}) = \int P_f(\boldsymbol{\vartheta}_{ij}, \boldsymbol{\vartheta}^*_{-ij}, \boldsymbol{y}) f_{\mathbf{y}}(\boldsymbol{y}) d\boldsymbol{\vartheta}_{-ij} d\boldsymbol{y} - P_{f\vartheta_i}(\vartheta_i) - P_{f\vartheta_j}(\vartheta_j) - P_{f0} \\ P_{f\boldsymbol{y}_{ij}}(\boldsymbol{y}_{ij}) = \int P_f(\boldsymbol{\vartheta}^*, \boldsymbol{y}) f_{\mathbf{y}_{-ij}}(\boldsymbol{y}_{-ij}) d\boldsymbol{y}_{-ij} - P_{fy_i}(y_i) - P_{fy_j}(y_j) - P_{f0} \\ P_{f\vartheta_i y_j}(\vartheta_i, y_j) = \int P_f(\vartheta_i, \boldsymbol{\vartheta}^*_{-i}, \boldsymbol{y}) f_{\mathbf{y}_{-j}}(\boldsymbol{y}_{-j}) d\boldsymbol{y}_{-j} - P_{f\vartheta_i}(\vartheta_i) - P_{fy_j}(y_j) - P_{f0} \end{cases} \tag{5}$$

where $\boldsymbol{\vartheta}^*$ means the fixed point of $\boldsymbol{\vartheta}$ chosen as the mid-point of $D_{\boldsymbol{\vartheta}}$ in this study. Unbiased estimators of each component function in Eq. (5) are then derived using the joint sample set $W = \{\boldsymbol{x}^{(k)}, \boldsymbol{y}^{(k)}\}$, for $k = 1,2,\cdots,N$, as:

$$\begin{cases} \hat{P}_{f0} = \frac{1}{N}\sum_{k=1}^{N} I_F\left(\boldsymbol{x}^{(k)}, \boldsymbol{y}^{(k)}\right) \\ \hat{P}_{f\vartheta_i}(\vartheta_i) = \hat{P}_{f0} r_{\vartheta_i}\left(\boldsymbol{x}^{(k)} \middle| \vartheta_i, \boldsymbol{\vartheta}^*_{-i}\right) \\ \hat{P}_{fy_i}(y_i) = \hat{P}_{f0} r_{y_i}(y_i|F,W) \\ \hat{P}_{f\boldsymbol{\vartheta}_{ij}}\left(\boldsymbol{\vartheta}_{ij}\right) = \hat{P}_{f0} r_{\boldsymbol{\vartheta}_{ij}}\left(\boldsymbol{x}^{(k)} \middle| \boldsymbol{\vartheta}_{ij}, \boldsymbol{\vartheta}^*_{-ij}\right) \\ \hat{P}_{f\boldsymbol{y}_{ij}}\left(\boldsymbol{y}_{ij}\right) = \hat{P}_{f0} r_{\boldsymbol{y}_{ij}}\left(\boldsymbol{y}_{ij}|F,W\right) \\ \hat{P}_{f\vartheta_i y_j}(\vartheta_i, y_j) = \left[\hat{P}_{f\vartheta_i}(\vartheta_i) + \hat{P}_{f0}\right] r_{y_j}(y_j|F,W) - \hat{P}_{f\boldsymbol{y}_j}(y_j) \end{cases} \tag{6}$$

where

$$\begin{cases} r_{\vartheta_i}\left(\boldsymbol{x}^{(k)} \middle| \vartheta_i, \boldsymbol{\vartheta}^*_{-i}\right) = \dfrac{f_{\mathbf{x}}\left(\boldsymbol{x}^{(k)} \middle| \vartheta_i, \boldsymbol{\vartheta}^*_{-i}\right)}{f_{\mathbf{x}}\left(\boldsymbol{x}^{(k)} \middle| \boldsymbol{\vartheta}^*\right)} - 1 \\ r_{y_i}\left(y_i \middle| F, W'\right) = \dfrac{\hat{f}_{y_i}(y_i|F,W)}{f_{y_i}(y_i)} - 1 \\ r_{\boldsymbol{\vartheta}_{ij}}\left(\boldsymbol{x}^{(k)} \middle| \boldsymbol{\vartheta}_{ij}, \boldsymbol{\vartheta}^*_{-ij}\right) = \dfrac{f_{\mathbf{x}}\left(\boldsymbol{x}^{(k)} \middle| \boldsymbol{\vartheta}_{ij}, \boldsymbol{\vartheta}^*_{-ij}\right)}{f_{\mathbf{x}}\left(\boldsymbol{x}^{(k)} \middle| \boldsymbol{\vartheta}^*\right)} - \dfrac{f_{\mathbf{x}}\left(\boldsymbol{x}^{(k)} \middle| \vartheta_i, \boldsymbol{\vartheta}^*_{-i}\right)}{f_{\mathbf{x}}\left(\boldsymbol{x}^{(k)} \middle| \boldsymbol{\vartheta}^*\right)} - \dfrac{f_{\mathbf{x}}\left(\boldsymbol{x}^{(k)} \middle| \vartheta_j, \boldsymbol{\vartheta}^*_{-j}\right)}{f_{\mathbf{x}}\left(\boldsymbol{x}^{(k)} \middle| \boldsymbol{\vartheta}^*\right)} + 1 \\ r_{\boldsymbol{y}_{ij}}\left(\boldsymbol{y}_{ij} \middle| F, W'\right) = \dfrac{\hat{f}_{\mathbf{y}_{ij}}(\boldsymbol{y}_{ij}|F,W)}{f_{\mathbf{y}_{ij}}(\boldsymbol{y}_{ij})} - \dfrac{\hat{f}_{y_i}(y_i|F,W)}{f_{y_i}(y_i)} - \dfrac{\hat{f}_{y_j}(y_j|F,W)}{f_{y_j}(y_j)} + 1 \end{cases} \tag{7}$$

are regarded as weight coefficients, where $\hat{f}_{y_i}(y_i|F,W)$ and $\hat{f}_{\mathbf{y}_{ij}}\left(\boldsymbol{y}_{ij}|F,W\right)$ denote the conditional PDFs of y_i and $\boldsymbol{y}_{ij}$, respectively, on the failure domain F estimated using the sample set W. The readers can refer to Ref. [7] for the detailed derivations of these conditional PDFs. It is noted that, to generate the joint sample set W, an auxiliary PDF of $\boldsymbol{y}$, $f_{\mathbf{y}}(\boldsymbol{y}) = \prod_{i=1}^{m} f_{y_i}(y_i)$, is necessary. Without loss of generality, we assume that each y_i follows a uniform distribution on its relaxed interval domain $\left[\underline{y}_i - \delta\Delta y_i, \overline{y}_i + \delta\Delta y_i\right]$, where Δy_i indicates the difference of the original interval and δ is a given value (e.g., $\delta = 0.2$), to improve the estimation performance around the original bounds [7]. Finally, sensitivity indices are proposed as follows for measuring the relative importance of the component functions:

$$S_{(\cdot)} = \frac{\mathrm{V}\left[P_{f(\cdot)}(\cdot)\right]}{\mathrm{V}\left[P_f(\boldsymbol{\vartheta}, \boldsymbol{y})\right]} \tag{8}$$

with

$$\begin{aligned} \mathrm{V}\left[P_f(\boldsymbol{\vartheta}, \boldsymbol{y})\right] = & \sum_{i=1}^{4n} \mathrm{V}\left[P_{f\vartheta_i}(\vartheta_i)\right] + \sum_{i=1}^{m} \mathrm{V}\left[P_{fy_i}(y_i)\right] + \sum_{i=1}^{4n-1}\sum_{j=i+1}^{2n} \mathrm{V}\left[P_{f\boldsymbol{\vartheta}_{ij}}\left(\boldsymbol{\vartheta}_{ij}\right)\right] \\ & + \sum_{i=1}^{m-1}\sum_{j=i+1}^{m} \mathrm{V}\left[P_{f\boldsymbol{y}_{ij}}\left(\boldsymbol{y}_{ij}\right)\right] + \sum_{i=1}^{4n}\sum_{j=1}^{m} \mathrm{V}\left[P_{f\vartheta_i y_j}\left(\vartheta_i, y_j\right)\right] + \cdots + \mathrm{V}\left[P_{f\boldsymbol{\vartheta}\boldsymbol{y}}(\boldsymbol{\vartheta}, \boldsymbol{y})\right] \end{aligned}$$

where V denotes the variance operator. The sensitivity indices measure the average L^2 distance of the components to the fixed point $\boldsymbol{\vartheta}^*$. The smaller the distance is, the less influential the component is.

The detailed procedure of the hybrid NISS method is shown in Fig.2. The statistical error of the NISS estimators is assessed by the bootstrap scheme. Let n_{boot} indicate the number of total bootstrap replications, we can obtain n_{boot} estimates of each component function and sensitivity index, and can calculate the confidence intervals $\left[\underline{\hat{P}}_{f(\cdot)}, \overline{\hat{P}}_{f(\cdot)}\right]$, e.g., $\left[\mathrm{E}\left[\hat{P}_{f(\cdot)}\right] - 2\left(\mathrm{V}\left[\hat{P}_{f(\cdot)}\right]\right)^{1/2}, \mathrm{E}\left[\hat{P}_{f(\cdot)}\right] + 2\left(\mathrm{V}\left[\hat{P}_{f(\cdot)}\right]\right)^{1/2}\right]$, where E is the mean operator, since the NISS estimators follow Gaussian distributions. We propose to estimate two coefficients of variations (CV), i.e., CVs at the points where $\underline{\hat{P}}_{f(\cdot)}$ returns the minimum and maximum values, $\mathrm{CV}_{\min\left(\underline{\hat{P}}_{f(\cdot)}\right)}$ and $\mathrm{CV}_{\max\left(\overline{\hat{P}}_{f(\cdot)}\right)}$. If their larger value is less than a given tolerance ε, the statistical error is acceptable, and if not, one should enrich the size of the joint sample set N. The truncation error on the other hand is quantified by the sensitivity indices. The components sensitivity indices of which are less than a threshold S_{thr} are ignored, and the resultant truncation error can be accepted if the summation of the sensitivity indices for all the components used is larger than a given threshold ϵ. Otherwise, one should decrease S_{thr}. Finally, the failure probability function $P_f(\boldsymbol{\vartheta}, \boldsymbol{y})$ is approximated as synthetic of all the influential component functions. One can also estimate the failure probability bounds by sampling methods, where not only the mean estimators but also the variance estimators can be evaluated within the bootstrap scheme.

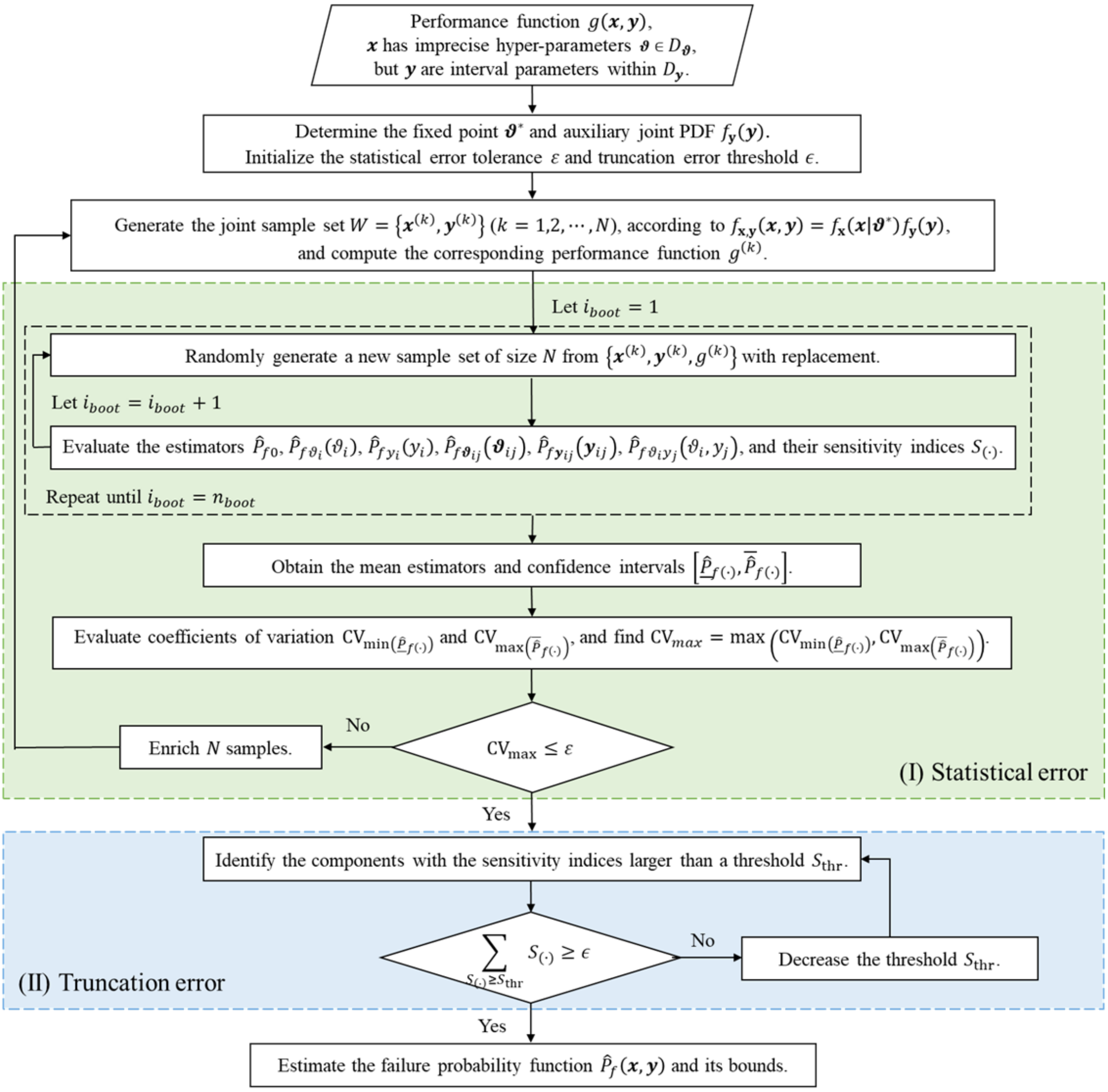

Fig. 2. Flowchart of the hybrid NISS method.

4. NASA UQ challenge problem 2019

The NASA UQ challenge problem 2019 [10] is investigated to demonstrate the capabilities of the proposed method. Fig. 3 shows the overall structure of Sub-problem C (Reliability analysis of baseline design). The model inputs consist of the five aleatory parameters $\boldsymbol{a} = (a_1, a_2, \cdots, a_5)^T$, four epistemic parameters $\boldsymbol{e} = (e_1, e_2, \cdots, e_4)^T$, and pre-specified design variable $\theta_{baseline}$ with nine components. The aleatory parameters are modeled by p-boxes while the epistemic parameters are modeled by intervals, based on the results of the first two subproblems, i.e., Sub-problem A (Model calibration & UQ of the subsystem) and Sub-problem B (Uncertainty reduction). It is important to note that, the distribution families of each aleatory parameter are completely unknown a priori. The reliability requirements of interest are represented by three limit state functions, i.e., a black-box function $g_1(\boldsymbol{a}, \boldsymbol{e}, \theta_{baseline}) < 0$,

$$g_2 = \max_{t\in[T/2,T]} |z_1(\boldsymbol{a}, \boldsymbol{e}, \theta_{baseline}, t)| - 0.02 < 0 \tag{9}$$

with a black-box time-independent output z_1, and

$$g_3 = \max_{t\in[0,T]} |z_2(\boldsymbol{a}, \boldsymbol{e}, \theta_{baseline}, t)| - 4 < 0 \tag{10}$$

with a black-box time-independent output z_2. The worst-case limit state function is then defined as:

$$\omega(\boldsymbol{a}, \boldsymbol{e}, \theta_{baseline}) = \max_{i=1,2,3} g_i(\boldsymbol{a}, \boldsymbol{e}, \theta_{baseline}) \tag{11}$$

The safe domain of the system is determined by the $\boldsymbol{a}$ points where $\omega(\boldsymbol{a}, \boldsymbol{e}, \theta_{baseline}) < 0$, whereas its complement set is accounted for as the failure domain.

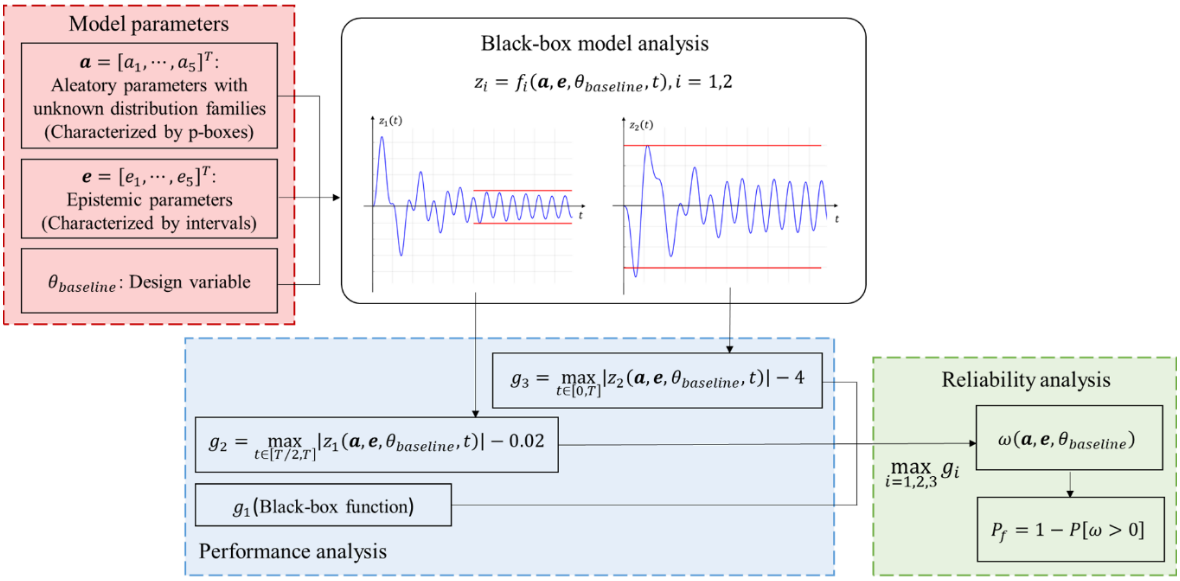

Fig. 3. Schematic of the NASA UQ challenge 2019 Sub-problem C.

Some of the authors have addressed the first two subproblems and have represented the aleatory parameters by the staircase distribution-based p-boxes [12]. We herein use the results in Ref. [12] for uncertainty characterization of $\boldsymbol{a}$ and $\boldsymbol{e}$, as summarized in Table 1. Under this assumption, 20 hyper-parameters of the staircase distributions are additionally employed as epistemic parameters, and thus totally 24 epistemic parameters (i.e., $\vartheta_i = \{\mu_i, m_{2i}, \tilde{m}_{3i}, \tilde{m}_{4i}\}$, for $i = 1, \cdots, 5$, and $\boldsymbol{e}$) are investigated in the reliability analysis. Each auxiliary PDF $f_{e_i}(e_i)$ is assumed as a uniform distribution on its relaxed intervals as shown in parentheses after the true intervals in Table 1. The parameters of the proposed method are set as $N = 5 \times 10^5$ and $n_{boot} = 20$, $\varepsilon = 0.15$ and, $\epsilon = 0.9$, respectively.

Table 1. Model parameters of the NASA UQ challenge problem.

Parameter	Uncertainty characteristic
a_1	Staircase distribution, $\mu_1 \in [0.5050, 0.5980]$, $m_{21} \in [0.0200, 0.0750]$, $\tilde{m}_{31} \in [0.9800, 1.4550]$, $\tilde{m}_{41} \in [4.0790, 6.3690]$
a_2	Staircase distribution, $\mu_1 \in [1.1110, 1.2290]$, $m_{21} \in [0.0660, 0.0670]$, $\tilde{m}_{31} \in [-0.6640, -0.2440]$, $\tilde{m}_{41} \in [3.7760, 4.9680]$
a_3	Staircase distribution, $\mu_1 \in [0.8040, 0.8720]$, $m_{21} \in [0.0300, 0.0440]$, $\tilde{m}_{31} \in [-0.9620, -0.6080]$, $\tilde{m}_{41} \in [3.7140, 3.7150]$
a_4	Staircase distribution, $\mu_1 \in [0.7870, 1.2050]$, $m_{21} \in [0.3520, 0.3530]$, $\tilde{m}_{31} \in [-0.7430, 0.2340]$, $\tilde{m}_{41} \in [1.4030, 2.5000]$
a_5	Staircase distribution, $\mu_1 \in [0.8510, 1.2240]$, $m_{21} \in [0.2390, 0.3690]$, $\tilde{m}_{31} \in [-0.5430, 0.4370]$, $\tilde{m}_{41} \in [1.3040, 3.0480]$
e_1	Interval, $e_1 \in [0.4674, 0.6433]$ (Relaxed interval $[0.2674, 0.8433]$)
e_2	Interval, $e_2 \in [0.7607, 0.9736]$ (Relaxed interval $[0.5607, 1.1736]$)
e_3	Interval, $e_3 \in [0.2865, 0.4583]$ (Relaxed interval $[0.0865, 0.6583]$)
e_4	Interval, $e_4 \in [0.9627, 1.1664]$ (Relaxed interval $[0.7627, 1.3664]$)

The mean value and standard deviation of the constant component estimator $\hat{P}_{f0}$ are computed as 0.1646 and 4.4×10^{-4}, respectively. The mean estimators of the first-order component functions as well as their 95.45 % confidence intervals are shown in Fig.4 for the hyper-parameters of the aleatory parameters $\boldsymbol{a}$ and in Fig.5 for the interval parameters $\boldsymbol{e}$. It can be seen that the confidence interval of each component function is narrow enough, indicating all the 24 component functions are accurately estimated using the proposed method. Similarly, among the second-order component functions, the mean estimators of the three most influential component functions are shown in Fig.6, together with their 95.45 % confidence intervals. As can be seen, these three second-order component functions are also effectively estimated with narrow confidence intervals.

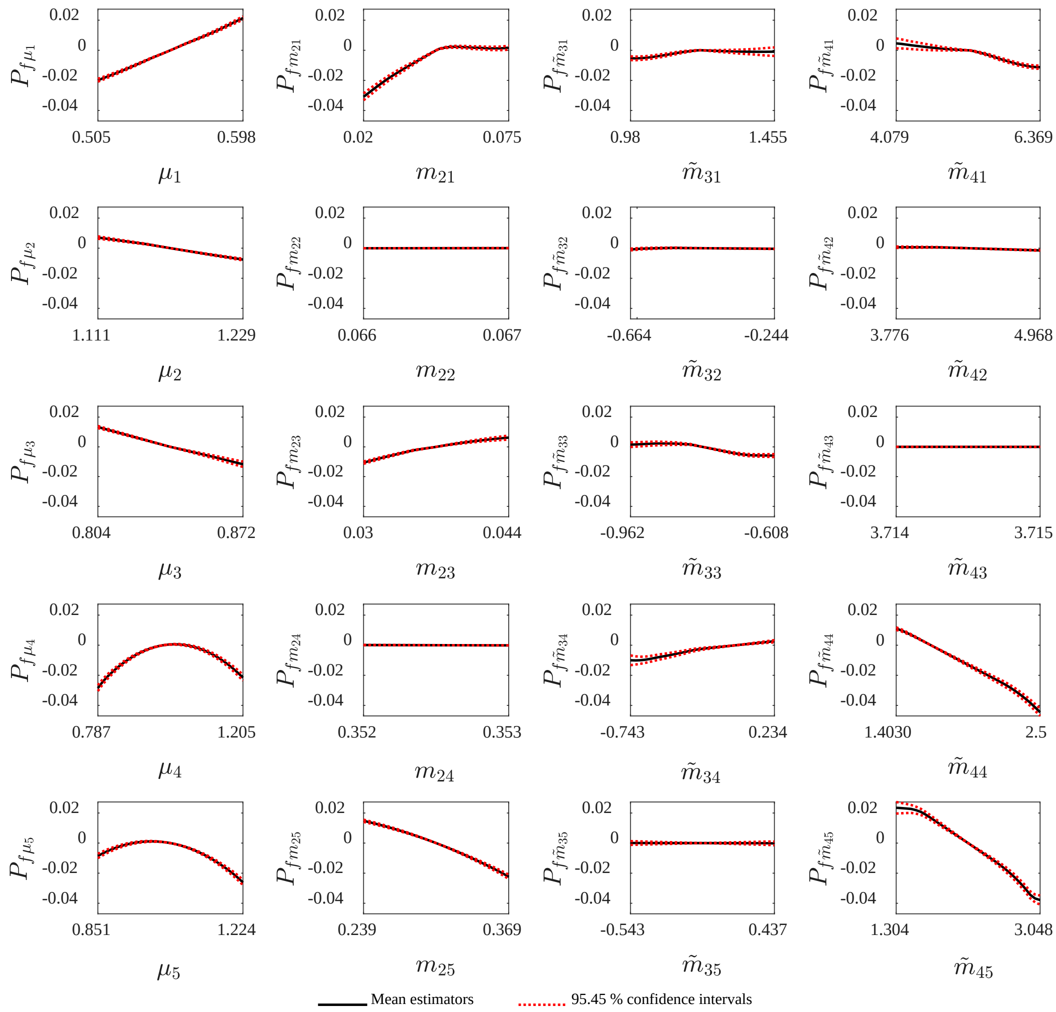

Fig. 4. First-order component functions of the hyper-parameters of $\boldsymbol{a}$.

We compute the sensitivity indices for all the first- and second-order component functions. The mean estimates as well as standard deviations are summarized in Table 2, for all the first-order and three most influential second-order component functions. It can be seen that all the sensitivity indices are accurately derived with small standard deviations. We assume that the component functions with the sensitivity indices larger than 0.01 are influential. Among the 24 first-order component functions, the eight components $\hat{P}_{f\mu_1}$, $\hat{P}_{fm_{21}}$, $\hat{P}_{f\tilde{m}_{44}}$, $\hat{P}_{f\tilde{m}_{45}}$, $\hat{P}_{fe_1}$, $\hat{P}_{fe_2}$, $\hat{P}_{fe_3}$, and $\hat{P}_{fe_4}$, and the three most influential second-order component functions $\hat{P}_{fe_1e_2}$, $\hat{P}_{fe_1e_3}$, and $\hat{P}_{fe_2e_3}$ are thus employed. The summation of the sensitivity indices of all these 11 components is larger than the threshold ϵ, implying the truncation error due to the truncation of the remaining components is acceptable. Finally, the failure probability function is approximated using the 11 influential components, and the failure probability bounds are estimated. The mean estimates and standard deviations are listed in Table 3. The results are compared with the reference bounds in Ref. [12] by the double-loop MCS [13] using the same parameter settings. It can be seen that both the upper and lower bounds show good agreement with the reference bounds.

Moreover, the total number of model evaluations of the hybrid NISS method is $N = 5 \times 10^5$, whereas that of the double-loop MCS is 5×10^6 [12]. Thus, the hybrid NISS method is ten times more efficient than the double-loop MCS. These outcomes demonstrate the feasibility of the hybrid NISS method in the propagation of mixed aleatory and epistemic uncertainties for the case where distribution families of the aleatory parameters are unknown.

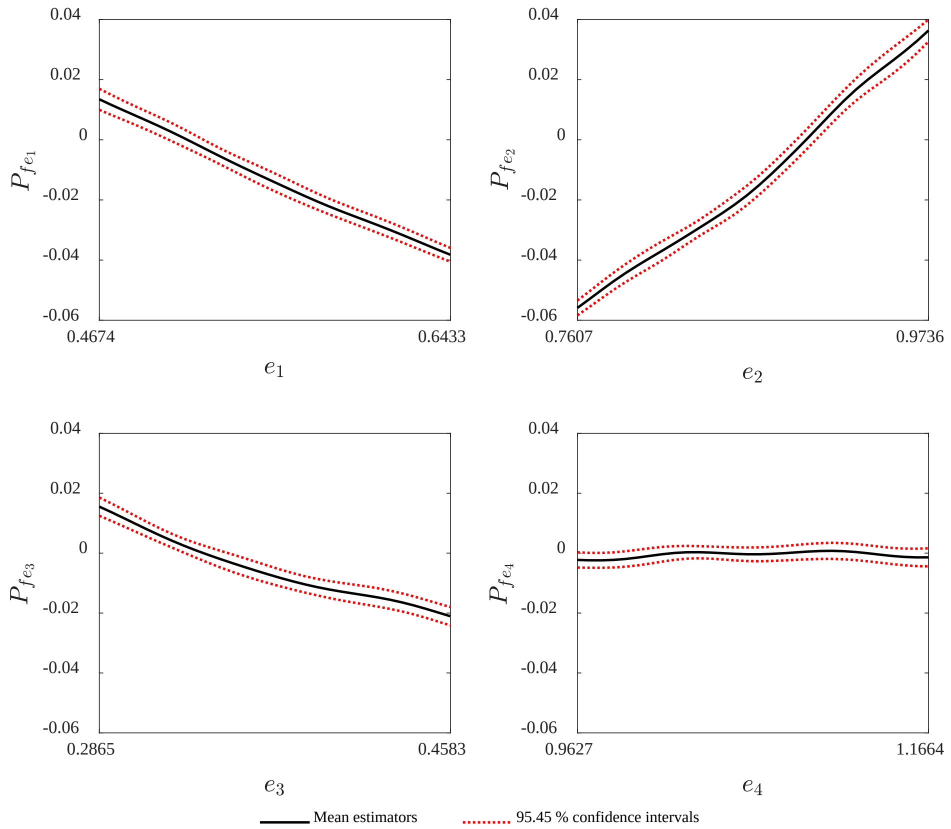

Fig. 5. First-order component functions of the epistemic parameters $\boldsymbol{e}$.

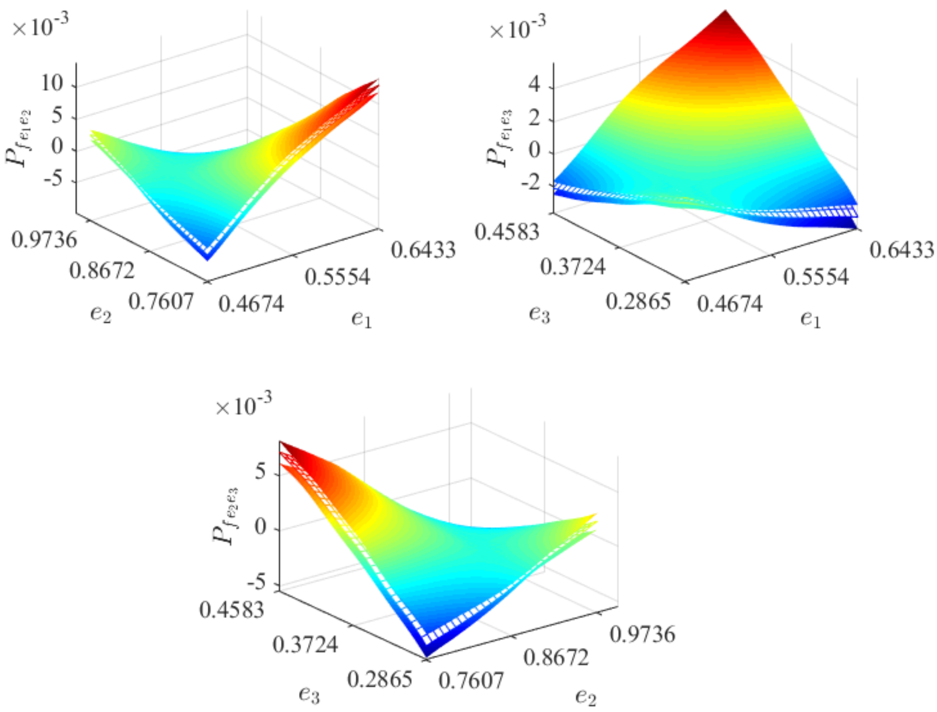

Fig. 6. The three most influential second-order component functions, where the in-between surfaces indicate the mean estimators and the other two surfaces indicate the 95.45 % confidence intervals.

Table 2. Sensitivity indices of the NASA UQ challenge problem.

	Mean estimate	Standard deviation		Mean estimate	Standard deviation
S_{μ_1}	0.0107	2.3×10^{-4}	$S_{\widetilde{m}_{34}}$	0.0018	3.0×10^{-4}
$S_{m_{21}}$	0.0121	3.2×10^{-4}	$S_{\widetilde{m}_{44}}$	0.0331	1.2×10^{-3}
$S_{\widetilde{m}_{31}}$	0.0006	4.9×10^{-5}	S_{μ_5}	0.0062	1.9×10^{-4}
$S_{\widetilde{m}_{41}}$	0.0027	1.6×10^{-4}	$S_{m_{25}}$	0.0087	2.3×10^{-4}
S_{μ_2}	0.0017	7.3×10^{-5}	$S_{\widetilde{m}_{35}}$	0.0000	1.8×10^{-6}
$S_{m_{22}}$	0.0000	9.3×10^{-9}	$S_{\widetilde{m}_{45}}$	0.0273	1.0×10^{-3}
$S_{\widetilde{m}_{32}}$	0.0000	2.2×10^{-6}	S_{e_1}	0.2202	3.8×10^{-3}
$S_{\widetilde{m}_{42}}$	0.0001	6.1×10^{-6}	S_{e_2}	0.4112	4.8×10^{-3}
S_{μ_3}	0.0047	5.0×10^{-4}	S_{e_3}	0.1044	2.0×10^{-3}
$S_{m_{23}}$	0.0019	2.0×10^{-4}	S_{e_4}	0.0213	5.7×10^{-4}
$S_{\widetilde{m}_{33}}$	0.0010	1.9×10^{-4}	$S_{e_1 e_2}$	0.0415	5.9×10^{-4}
$S_{\widetilde{m}_{43}}$	0.0000	2.1×10^{-10}	$S_{e_1 e_3}$	0.0105	2.9×10^{-4}
S_{μ_4}	0.0093	2.9×10^{-4}	$S_{e_2 e_3}$	0.0197	5.4×10^{-4}
$S_{m_{24}}$	0.0000	6.7×10^{-9}			

Table 3. Failure probability bounds of the NASA UQ challenge problem.

Parameter	Double-loop MC in Ref. [12]	Hybrid NISS method	
		Mean estimate	Standard deviation
Lower bound of P_f	0.0270	0.0299	0.0024
Upper bound of P_f	0.2746	0.2564	0.0030

5. Conclusions and discussions

This paper presents two contributions to effectively propagate the imprecise probability models without limiting hypotheses on the distribution family. First, the staircase distribution-based p-boxes are defined as a novel class of the parametric p-box. They can explicitly consider the imprecision not only in their hyper-parameters but also in the distribution families. Thus, they are especially suitable to characterize the true-but-unknown CDFs of the random variables whose distribution families are not known. Second, the novel hybrid NISS method is developed, in which the staircase distribution-based p-boxes are propagated by the locally expanded HDMR decomposition whereas the interval models are propagated by the globally expanded HDMR decomposition. This method can achieve a good balance between the efficiency in computing the NISS estimators for the hyper-parameters of the p-boxes and the global accuracy of those for the interval parameters. The NASA UQ challenge 2019 has demonstrated the effectiveness of the proposed method.

Acknowledgments

The first author acknowledges the support of the Deutsche Forschungsgemensschaft (DFG, German Research Foundation) — SFB1463-434502799.

References

1. A. Der Kiureghian, O. Ditlevsen, Aleatory or epistemic? Does it matter?, Struct. Safety 85 (2004) 11-19.
2. M. Faes, D. Moens, Recent trends in the modeling and quantification of non-probabilistic uncertainty, Arch. Comput. Methods Eng. 27 (2020) 633-671.
3. M. Beer, S. Ferson, V. Kreinovich, Imprecise probabilities in engineering analysis, Mech. Syst. Signal Process. 37 (2013) 4-29.
4. P. Wei, Z. Lu, J. Song, Extended Monte Carlo simulation for parametric global sensitivity analysis and optimization, AIAA J. 52(4) (2014) 867-878.

5. P. Wei, J. Song, S. Bi, M. Broggi, M. Beer, Z. Yue, Z. Lu, Non-intrusive stochastic analysis with parameterized imprecise probability models: I. Performance estimation, Mech. Syst. Signal Process. 124 (2019) 349-368.
6. P. Wei, J. Song, S. Bi, M. Broggi, M. Beer, Z. Yue, Z. Lu, Non-intrusive stochastic analysis with parameterized imprecise probability models: II. Reliability and rare events analysis, Mech. Syst. Signal Process. 126 (2019) 227-247.
7. J. Song, P. Wei, M. Valdebenito, S. Bi, M. Broggi, M. Beer, Z. Lu, Generalization of non-intrusive imprecise stochastic simulation for mixed uncertain variables, Mech. Syst. Signal Process. 134 (2019) 106316.
8. M. Faes, M. Daub, S. Marelli, E. Patelli, M. Beer, Engineering analysis with probability boxes: A review on computational methods, Struct. Safety 93 (2021) 102092.
9. L.G. Crespo, S.P. Kenny, D.P. Giesy, B.K. Stanford, Random variables with moment-matching staircase density function, Appl. Math. Modell. 64 (2018) 196-213.
10. L.G. Crespo, S.P. Kenny, The NASA langley challenge on optimization under uncertainty, Mech. Syst. Signal Process. 152 (2021) 107405.
11. R.B. Nelsen, An Introduction to Copulas; 2nd ed, Springer, New York, 2006.
12. A. Lye, M. Kitahara, M. Broggi, E. Patelli, Robust optimization of a dynamic black-box system under severe uncertainty: A distribution-free framework, Mech. Syst. Signal Process. 167 (2022) 108522.
13. R. Rocchetta, M. Broggi, E. Patelli, Do we have enough data? Robust reliability via uncertainty quantification, Appl. Math. Modell. 54 (2018) 710-721.